【論文】

Measurements of In-Plane Thermal Conductivity and Electrical Conductivity of Suspended Platinum Thin Film

懸架白金薄膜面方向の熱伝導率および電気伝導度の測定

Xing ZHANG*, Huaqing XIE*, Motoo FUJII*, Koji TAKAHASHI**
Hiroki AGO*, Tetsuo SHIMIZU***, Hidekazu ABE***

張　興*、謝 華清*、藤井丕夫*、高橋厚史**
吾郷浩樹*、清水哲夫***、阿部秀和***

As the first part in the measurements of the thermal conductivity of a single carbon nanotube by using the method with sample-attached T-type nanosensor, the electrical and thermal properties of the platinum (Pt) nanosensors have been investigated. The suspended Pt nanosensors with the thickness of 40 nm, the width of 360-600 nm, and the length of about 6.0 μm were fabricated with the electron beam lithography, electron beam physical vapor deposition and isotropic/anisotropic etching techniques. The electrical resistances of these nanosensors were measured by a four-wire method and the resistance-temperature coefficient was determined from the measured resistances at different temperatures. Based on one-dimensional heat conduction model, the in-plane thermal conductivity of the nanosensor was calculated from the linear relation of the volume-averaged temperature increase and the heating rate measured in vacuum. The experimental results show that the electrical conductivity, the resistance-temperature coefficient and the in-plane thermal conductivity of the nanosensor are much lower than those of the bulk values.

[**Keywords**: electrical conductivity, thermal conductivity, nanosensor, nanofilm]

本研究は定常短細線加熱法によるカーボンナノチューブの熱伝導率測定に関する研究の一部として、白金ナノプローブ自体の電気的および熱的特性を測定したものである。Si 基板に電子ビームリソグラフィによるパターン化、電子ビーム蒸着法による製膜およびエッチング処理などによって、厚さ 40 nm、幅 360-600 nm、長さ約 6 μmの懸架白金ナノプローブを製作した。10℃から 60℃の温度範囲でプローブの電気抵抗を測定し、懸架白金ナノプローブの電気抵抗の温度係数を求めた。さらに、真空中で通電加熱し、一次元熱伝導モデルを用いて、懸架白金薄膜面方向の熱伝導率を算出した。その結果、懸架白金薄膜面方向の熱伝導率および電気伝導度とその温度係数がバルクの値より大きく低下することが明らかになった。

* Institute for Materials Chemistry and Engineering, Kyushu University, Kasuga 816-8580, Japan. 九州大学先導物質化学研究所、〒816-8580 福岡県春日市春日公園６－１.
Fax: +81-92-583-7638　E-mail: xzhang@cm.kyushu-u.ac.jp

** Graduate School of Engineering, Kyushu University, Fukuoka 812-8581, Japan. 九州大学工学府、〒812-8581 福岡市東区箱崎 6-10-1. E-mail: takahashi@aero.kyushu-u.ac.jp

*** Nanotechnology Research Institute, National Institute of Advanced Industrial Science and Technology, Tsukuba 305-8562, Japan. 産業技術総合研究所ナノテクノロジー研究部門、〒305-8562 茨城県つくば市東１－１－１.
E-mail: tetsuo-shimizu@aist.go.jp

1. INTRODUCTION

Carbon nanotubes have attracted considerable attention since its discovery [1] due to their potential applications in electronic and energy conversion devices. The electrical and mechanical properties have been investigated at a single nanotube level. The thermal properties of carbon nanotubes are of fundamental interest as well as technological importance. However, most of the studies only include extracting the thermal properties of carbon nanotubes from the experiments of micrometer-/millimeter-sized mats of carbon nanotubes. Kim et al. [2] used a microfabricated suspended structures to probe the thermal transport of carbon nanotubes free from a substrate contact. However, it is hard to estimate the error in their measurements. We proposed a method using a sample-attached T-type nanosensor to measure the thermal conductivity of a single carbon nanotube. The method has been developed and successfully used to measure the thermal conductivity of one single carbon fiber [3]. In the measurements, the sample of a fiber/tube/wire as a pin fin is attached to a short hot wire that is supplied with a constant direct current to generate a uniform heat flux. Based on the analysis of one-dimensional steady-state heat conduction along the wire and the attached sample, the thermal conductivity of sample can be determined when the average temperature rise and the heat generation rate of the hot wire are measured. The method is regarded to have the advantages of simplicity as well as high accuracy. However, due to the small size of carbon nanotubes, the hot wire should be fabricated in a rather small size, like 100 nm, to obtain high sensitivity of the measurements. As known, the thermal and electrical properties of nanoscale materials are very different from bulk values due to the structure defect and boundary scattering [4-6]. Large error would take place if the bulk values were taken as the electrical and thermal properties for the nanosized hot-wire in the measurements and calculations. Therefore it is essential to determine the electrical and thermal properties for nanosensors in our experiments for measuring the thermal conductivity of one single carbon nanotube.

The objectives of the present work are to investigate the electrical and thermal properties of the nanosensors fabricated by electron beam (EB) lithography, electron beam physical vapor deposition (EBPVD) and isotropic/ anisotropic etching techniques. A four-wire method is used to measure the resistance and a one-dimensional heat conduction method is used to determine the thermal conductivity. Furthermore, natural convection heat transfer coefficient at atmospheric pressure is also investigated.

2. EXPERIMENTS

Figure 1 shows a schematic diagram of the nanosensor and the scanning electron microscope (SEM) image of the nanofilm marked by a circle in the left figure. Five nanosensors with the thickness of about 40 nm, the width of 360-600 nm, and the length of about 6.0 μm were made in the present study. The fabrication processes of the nanosensor are based on EB lithography, EBPVD and isotropic/anisotropic etching techniques as shown in Fig. 2. The details are listed as follows: (a) Si (100) substrate with SiO_2 layer of 180 nm thickness is used as starting material. EB resist is spin-coated to be 320 nm thick. (b) By using an electron beam lithography system, patterns of nano wires and leads are directly drawn on the EB resist. (c) Titanium and platinum films are deposited by EBPVD method. The thicknesses of titanium and platinum are 5 nm and 40 nm, respectively. Titanium film is used only for adhesion. (d) Lift-off technique is applied, where the chip is immersed in

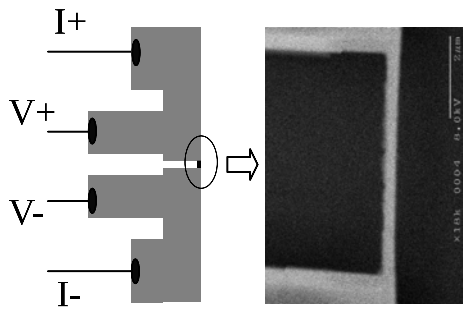

Fig.1. Schematic diagram of the nanosensor and SEM image of the suspended nanofilm.

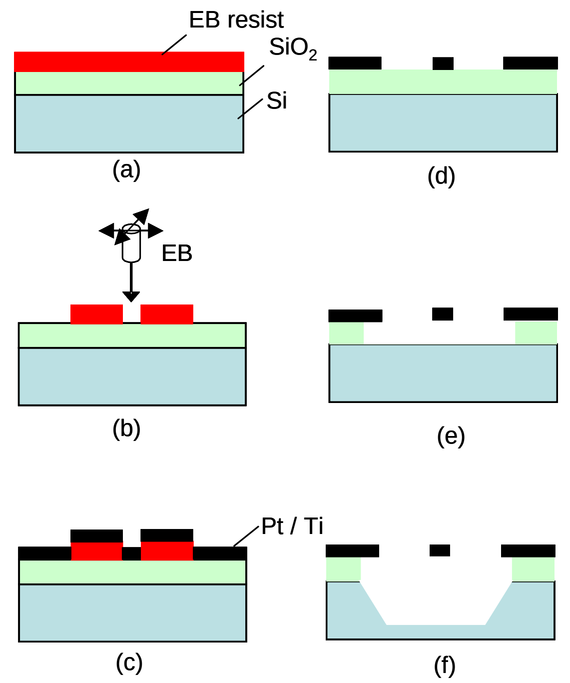

Fig. 2 Fabrication processes of nanosensor.

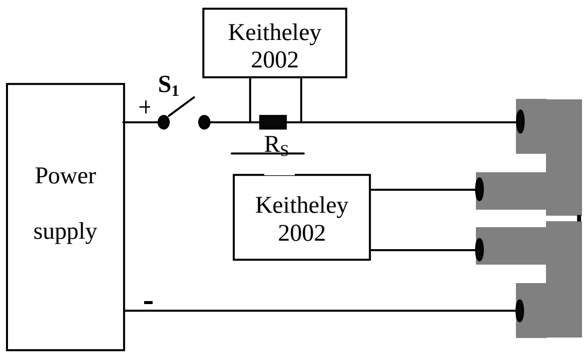

Fig. 3. Schematic drawing of the electrical circuit.

liquid resist-remover to leave Pt/Ti pattern only on SiO_2 layer. (e) Isotropic etching using buffered hydrofluoric acid is applied to remove SiO_2 layer around the nano Pt film. Titanium is also etched away in this process. (f) Si is anisotropically etched using KOH solution in order to detach the nanofilm from substrate. In the present study, the gap between the nanofilm and substrate is about 6 μm, and the Pt film is not etched by the buffered hydrofluoric acid and KOH solution.

Figure 3 shows an electrical circuit for measuring the electrical and thermal properties. In the measurements of the temperature coefficient of resistance, the silicon wafers with the nanosensors were placed in a constant temperature bath and the electrical resistances R, at different temperatures, were measured using a four-wire technique (see fig. 3). The resistance-temperature coefficient (β) is determined by the following formula.

$$\beta = \frac{R - R_0}{R_0 (T - T_0)} \tag{1}$$

Where R_0 is the resistance at temperature T_0.

In the measurements of the thermal properties, the nanosensor serves both as a heating source with homogeneous heat flux and as an electrical thermometer. Initially the nanosensor and its connectors keep at thermal equilibrium at T_0. When a constant heating current flows though the nanosensor, the nanosensor is heated and appears to be subjected to one-dimensional heat transfer. The physical model is shown in Fig. 4. The non-dimensional heat transfer equation is expressed as

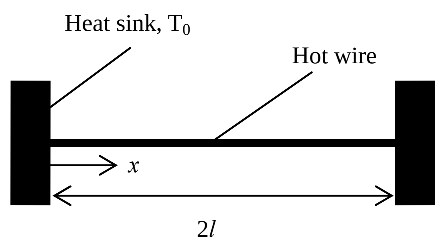

Fig. 4. Physical model of heat transfer in nanosensor.

$$\frac{\partial \theta}{\partial Fo} = \frac{\partial^2 \theta}{\partial X^2} - 2\eta Bi \theta + 1 \tag{2}$$

where $\theta = (T - T_0)/(q_v r_h^2/\lambda)$ is the dimensionless temperature rise, $Fo = \alpha t / r_h^2$ Fourier number, $r_h = \sqrt{(wd)/\pi}$ the specified radius, $Bi = h r_h / \lambda$ Biot number, $\eta = (w + d)/\pi r_h$ the shape factor, and $X = x / r_h$ the dimensionless length. In these dimensionless parameters, λ and α are the thermal conductivity and thermal diffusivity, respectively. l, w, and d are the half length, width, and thickness, respectively. q_v is the Joule heat per unit volume and h is the heat transfer coefficient which includes the effect of natural convection and radiation. The initial conditions are given as

$$Fo = 0 \qquad \theta = 0 \tag{3}$$

and the boundary conditions are given as

$$X = 0\,, \quad \theta = 0 \tag{4a}$$

and
$$X = L(L = l/r_h)\,, \quad \frac{\partial \theta}{\partial X} = 0 \tag{4b}$$

Equation (2) was solved numerically using a finite difference method under the above initial and boundary conditions. Calculated results show that the temperature distribution in a nanosensor with a specified radius 80 nm reaches steady-state after heated 4 μs, which indicates it is reasonable to adopt steady-state heat transfer in the nanosensor in our measurements. The radiation heat loss is negligible because the experiment temperature is only about 300 K. When the nanosensor is heated in a vacuum, there is no natural convection and the nanosensor appears as steady-state one-dimensional heat conduction. The analytical solution for equation (2) without transient term and convection term is obtained and the dimensionalized volume-averaged temperature rise (ΔT_V) is expressed by the heating rate (q), the sensor dimensions, and the thermal conductivity (λ) as

$$\Delta T_V = \frac{q}{\lambda} \times \frac{l}{6wd} \tag{5}$$

Therefore, the thermal conductivity is given as

$$\lambda = \frac{q}{\Delta T_V} \times \frac{l}{6wd} \tag{6}$$

Once the thermal conductivity of a nanosensor is determined from the relation between ΔT_V and q measured in vacuum, based on the analytical solution of equation (2) without transient term, the natural convection heat transfer coefficient can further be obtained from the relation between ΔT_V and q measured at a given pressure.

3. RESULTS AND DISCUSSION

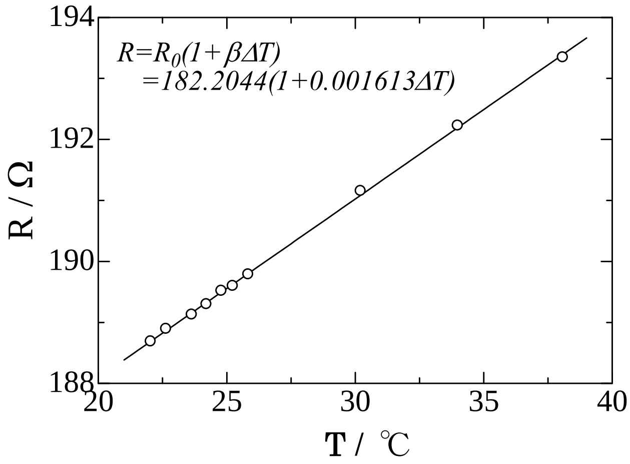

Fig. 5. Dependence of the resistance on the temperature.

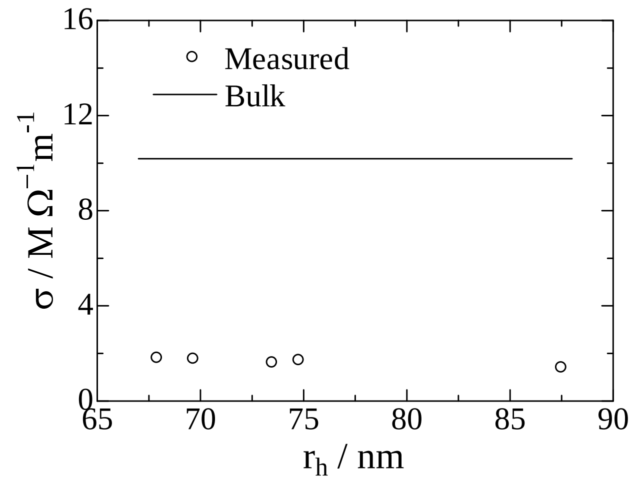

Fig. 6. Electrical conductivity of the nanosensor.

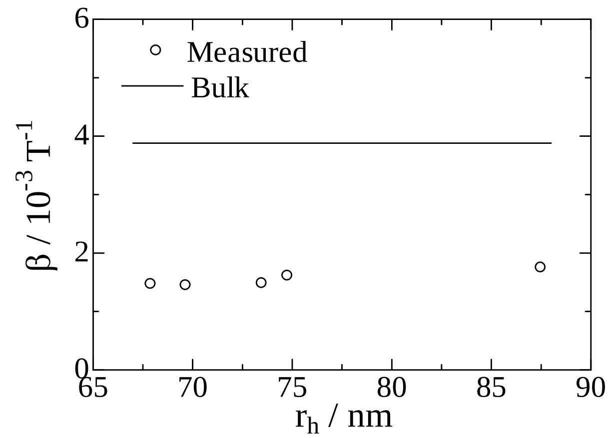

Fig. 7. Resistance-temperature coefficient of the nanosensor.

The linear relation between the electrical resistance and temperature is shown in Fig. 5. The electrical resistance at the corresponding temperature is measured by supplying a small current of about 7 μA to the nanosensor where the self-heating rate caused by the small current is about 8.9×10^{-9} W, and the temperature rise of the nanofilm even in vacuum is also below 0.0085 K. Using least-squares fit, the slope of R to T was determined and β was calculated by Eq. (1). The electrical conductivities σ of these five nanosensors and that of bulk platinum are presented in Fig. 6. It is seen that the bulk value of σ is much lager compared to the measured values for the nanosensors. The low values of the nanosensors might be attribured to the structure defect formed during fabrication and to the boundary scattering of electrons [7].

Figure 7 shows the resistance-temperature coefficients of the nanosensors and the bulk value. The resistance-temperature coefficient of the nanosensors, which is about 0.0015 K^{-1}, is less than half of that of the bulk value of 0.0039 K^{-1}.

When subjected to different current, the nanosensor is heated to different temperature that can be determined from the measurement of the electrical resistance using the following expression

$$\Delta T = \frac{R - R_0}{R_0 \beta} \tag{7}$$

The volume-averaged temperature rise of the nanosensor as a function of heating rate is shown in Fig. 8. It is clearly seen that the temperature rise at atmospheric pressure is much lower than that in vacuum at the same heating rate, indicating that the effect of natural convection is significant. The slope of ΔT_V to q is determined by linear fit of the experimental data and the thermal conductivity of nanosensor is determined from equation (6). The thermal conductivities of the five prepared nanosensors together with that of bulk value are presented in Fig. 9. It is obvious that the measured thermal conductivities of all the five nanosensors are much lower than that of bulk value. The bulk value of the thermal conductivity of Pt is 71.4 $Wm^{-1}K^{-1}$, whereas those of the experiments are 27.7~33.6 $Wm^{-1}K^{-1}$,

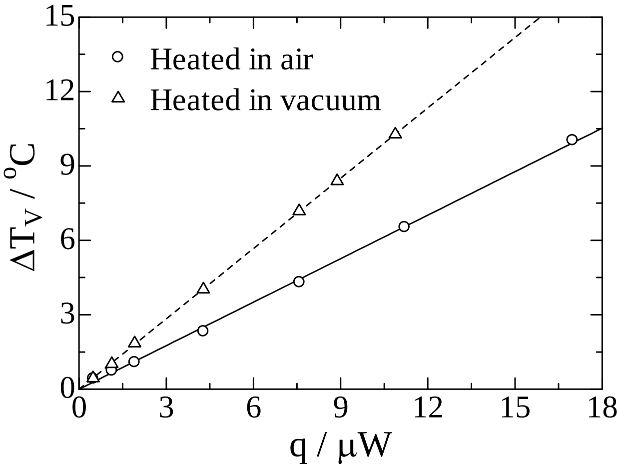

Fig. 8. Temperature rise as a function of heating rate.

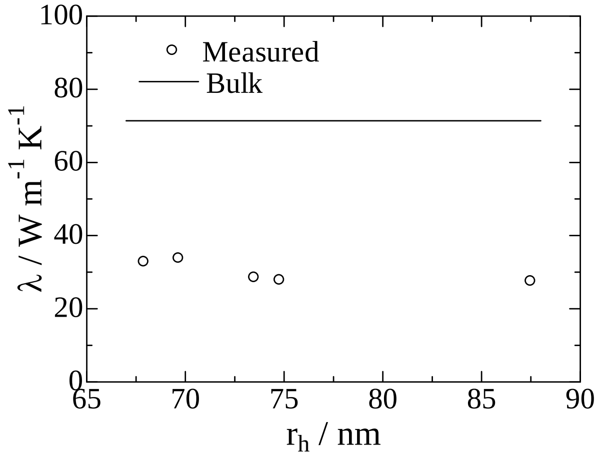

Fig. 9. Thermal conductivity of the nanosensor.

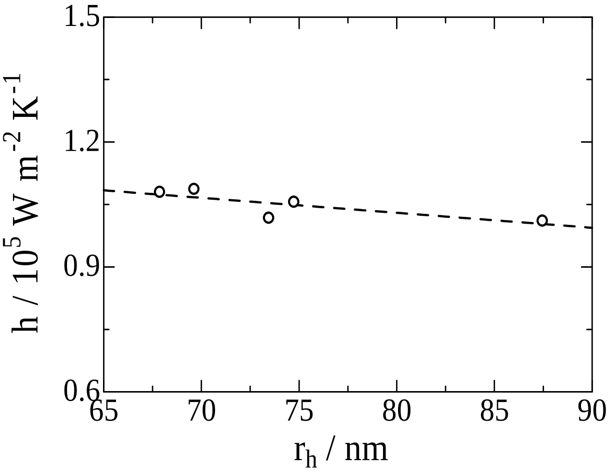

Fig. 10. Heat transfer coefficient of the nanosensor.

less than half of the bulk value. The error of the thermal conductivity might come from the measurement errors of voltage, current, temperature, and the dimensions of the nanosensor. The width and length of the nanosensor are measured with a scanning electron microscope and the film thickness is measured with a calibrated quartz crystal thin-film thickness monitor (CRTM-7000 with the resolution of 0.01 nm). The error caused by the dimension measurements is estimated to be less than $\pm 3\%$. Therefore, the total error of the thermal conductivity is estimated to be within $\pm 5\%$. It is worth to note that the ratio of the thermal conductivity to the electrical conductivity is calculated from measured values to be about 1.5×10^{-5} W Ω K^{-1}, whereas that of the bulk platinum is about 7.0 $\times 10^{-6}$ W Ω K^{-1}. This remarkable discrepancy indicates that the relation between thermal conductivity and electrical conductivity of these nanoscale thin films appears not to follow the Wiedemann-Franz law which determines the relation between the thermal conductivity and electrical conductivity of a bulk metallic materials. The low values of the thermal and electrical properties for the thin-films could be attributed to the structure defect, surface scattering, grain boundary scattering, film sizes, fabrication methods and etc. Because it is very difficult to determine which is the main cause of the low values, the measured thermal and electrical properties are regarded as the special values for the present nanosensors.

The natural convection heat transfer coefficients at atmosphere pressure are shown in Fig. 10. The dashed line in Fig. 10 is only for guide eyes. Nanosensors have very large convective heat transfer coefficients, indicating that a surface with smaller scale can cause higher effect of natural convection heat transfer.

4. CONCLUSIONS

The thermal and electrical properties of the suspended platinum thin film nanosensors have been investigated. The in-plane thermal conductivities of these films were shown to less than half of the bulk value. The nanoscale thin films have significantly lower electrical conductivity than bulk platinum. Also the resistance-temperature coefficients of these nanosensors are much smaller compared to the bulk data. On the other hand, the natural convection heat transfer coefficients are high. These measurements enable us to proceed to the measurements of the thermal conductivity of a single carbon nanotube.

ACKNOWLEDGMENTS

This work is supported partly by the Grant-in-Aid for Scientific Research B15360114 from the Ministry of Education, Science, Sports and Culture of Japan.

REFERENCES

[1] S. Iijima, Nature, **354** (1991), 56.

[2] P. Kim, L. Shi, A. Majumdar, and P. L. McEuen, Physical Review Letters, **81** (2001), 215502.

[3] X. Zhang, S. Fujiwara, and M. Fujii, International Journal of Thermophysics, **21** (2000), 965.

[4] S. R. Mirmira and L. S. Fletcher, Journal of Thermophysics and Heat Transfer, **12** (1998), 121.

[5] D. G. Cahill, W. K. Ford, K. E. Goodson, G. D. Mahan, A. Majumdar, H. J. Maris, R. Merlin, and S. Phillpot, Journal of Applied Physics, **93** (2003), 793.

[6] T. Yamane, S. Katayama, and M. Todoki, Proceedings of the 24th Japan Symposium on Thermophysical Properties, 2003, Okayama, pp. 26.

[7] S. Kumar, G. C. Vradis, Journal of Heat Transfer, **116** (1994), 28.

[Received Nov. 11, 2004, Accepted Jan. 18, 2005]